January 2009 *Volume 5 Issue 1*

Trade Science Inc.

Materials Science

An Indian Journal

Full Paper

MSAIJ, 5(1), 2009 [29-35]

Electrical properties of alizarin doped anthraquinone: Impedance spectroscopy analysis

K.P.Chandra[1], L.N.Mandal[2], K.Prasad[3]*

[1]Department of Physics, S.M.College, Bhagalpur, 812001, (INDIA)

[2]Department of Physics, Murarka College, Sultanganj, Bhagalpur, 813213, (INDIA)

[3]University Department of Physics, T.M.Bhagalpur University, Bhagalpur, 812007, (INDIA)

E-mail: k.prasad65@gmail.com

PACS: 72.80.Le; 72.20.-i; 77.22.Gm; 81.05.Hd.

Received: 8th October, 2008 ; Accepted: 13th October, 2008

ABSTRACT

The electrical properties of organic mixture anthraquinone-0.6% alizarin were investigated by the complex impedance spectroscopy technique. A transition from semiconducting to conducting state is observed. The dielectric relaxation is found to be of non-Debye type. Evidences of temperature-dependent electrical relaxation phenomena and negative temperature coefficient of resistance (NTCR) character of the sample are observed. The ac conductivity obeys the power law. AC conductivity analysis indicated the possibility of hopping mechanism for electrical transport processes in the system. The activation energy, density of states at Fermi level and minimum hopping distance are estimated from ac conductivity data.

KEYWORDS

Organic semiconductor;
Impedance;
Electrical conductivity;
Dielectric relaxation.

INTRODUCTION

Organic materials exhibiting semiconducting properties are technologically important as an alternative to inorganic semiconductors, e.g. Si, GaAs, etc.[1]. Organic semiconductors (OSCs) are successfully used in transistors[2-5], electroluminescence[6], light emitting diodes[7], lasers[8], active pixels colour display[1], etc. In OSCs free electron-hole pairs are generated from thermal and/or photon excitation which allow carrier transport. OSCs show the characteristic feature of being rich of π-orbitals. These orbitals give rise to states delocalized over the single macromolecule. The electron transport properties in organic compounds are mainly due to the weak interaction among π-orbitals of different macromolecules. In recent years, the charge carrier transport properties and charge injection mechanisms in OSCs have received considerable attention as they follow different aspects of conduction mechanism. Also, they have capability to support electronic conduction. This is because transport of the charge carriers at dc or at very low frequencies requires a kind of percolation network of transition, in which the weakest links (intra-chain connection) determine magnitude of the conductivity[5]. At higher frequencies, the charge carriers become localized in small regions of low energy barrier[9]. Therefore, complex impedance spectroscopy technique is considered to be an appropriate and effective tool to understand the charge transport, dielectric relaxation and conduction mechanisms in OSCs[10]. The charge transport in OSCs can be due to the charge displacement, dipole reorientation (charge hopping) and space

charge formation[11]. Charge transport process causes a number of different polarization mechanisms that results frequency dispersion or in the materials under an ac field[12]. Extensive literature survey indicated that only a few experimental results on electrical impedance study of OSCs have been reported so far[5,13-18]. In this work, ac electrical response of organic mixture anthraquinine-0.6% alizarin (abbreviated hereafter AQAL) has been reported. The conduction mechanism and dielectric relaxation have also been evaluated.

EXPERIMENTAL

The AR grade anthraquinone and 0.6% alizarin (NBS Biologicals, England) by weight were mixed and pressed into a circular disc shaped pellets (diameter 9.98 mm and thickness 1.22 mm) under a uniaxial stress of 5 MPa. The pellets were then heated at 150^{0}C for 2hrs. The electrical measurements were carried out on a symmetrical cell of type Ag | AQAL | Ag, where Ag is a conductive paint coated on either side of the pellet. Electrical impedance (Z), phase angle (θ) and loss tangent (tanδ) were measured as a function of frequency (0.1 kHz-1 MHz) at different temperatures (30^{0}C-110^{0}C) using a computer-controlled LCR Hi-Tester (HIOKI 3532-50, Japan) with a microprocessor based low temperature furnace (DPI-1100), Sartech Intl. India.

RESULTS AND DISCUSSION

Figures 1 and 2 respectively, show the frequency dependence of dielectric constant (ε) and dielectric loss (tanδ) at several temperatures. Plots illustrate the inverse dependence of ε on frequency. Also, the loss spectrum shows a peak at all the temperatures. The room temperature value of ε and tanδ at 1 kHz were found respectively to be 214 and 0.63. Further, both the pattern presents the dispersion in the lower frequency. This is due to the fact that dipoles can no longer follow the field at high frequencies. Further, it is observed that the values of both ε and tanδ increases up to 50ºC and then they decreases (inset figures 1 and 2) i.e. system shows phase transition, T_c from semiconducting to conducting state[19,20]. The gradual fall in the values both ε

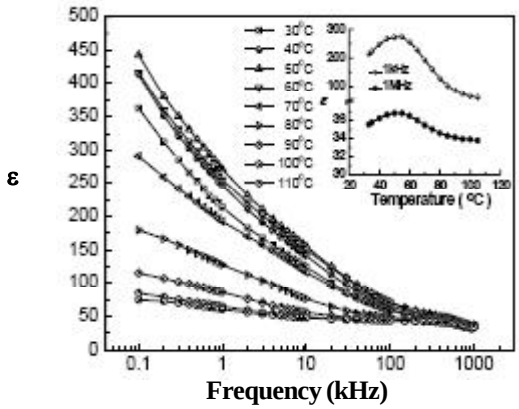

Figure 1: Frequency dependence of dielectric constant of anthraquinone-0.6% alizarin at different temperatures. Inset: Variation of ε with temperature at 1kHz and 1MHz

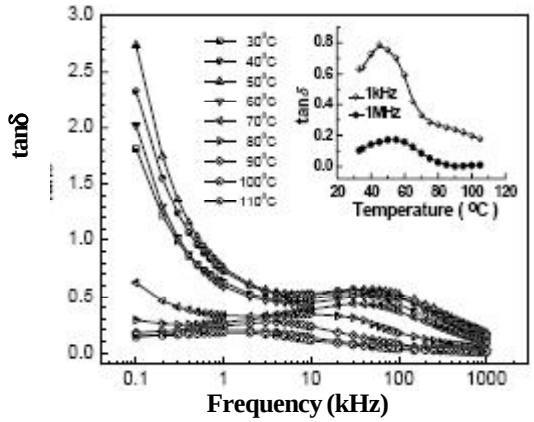

Figure 2: Frequency dependence of tanδ of anthraquinone-0.6% alizarin at different temperatures. Inset: Variation of tanδ with temperature at 1kHz and 1MHz

and tanδ with temperature may possibly be due to the electrical conductivity of the materials that modifies the value of the capacitance as the temperature increases. Besides, it is known that there are pronounced effect of frequency as well as temperature on the electrical conduction and dielectric relaxations of a material. Also, the loss tangent in a system is defined as tan $\delta = \varepsilon'' / \varepsilon'$ where ε' is real and ε'' is imaginary part of dielectric constant. It is evident from figure 2 that at loss spectrum consists of two components: the conductivity response of free charges (i.e. $\varepsilon'' = \sigma/\omega\varepsilon_0$) and the frequency dependent polarization loss response of dipoles (relaxation part). Therefore, the complete dielectric response in such case, can be expressed as:

$$\varepsilon = \varepsilon' - \mathbf{i}(\varepsilon'' + \sigma / \omega\varepsilon_0)$$

Figures 3 and 4 respectively, show respectively the

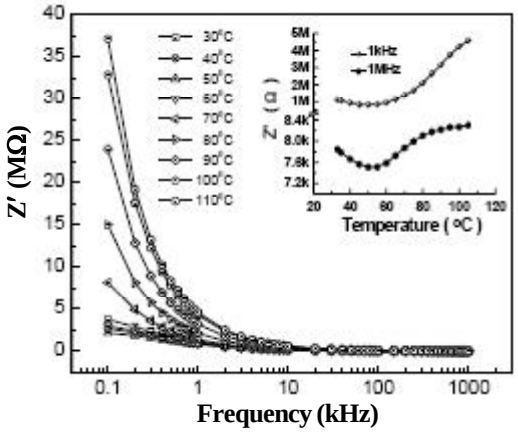

Figure 3: Frequency dependence of real part of impedance of anthraquinone-0.6% alizarin at different temperatures. Inset: Temperature dependence of real part of impedance at 1kHz and 1MHz

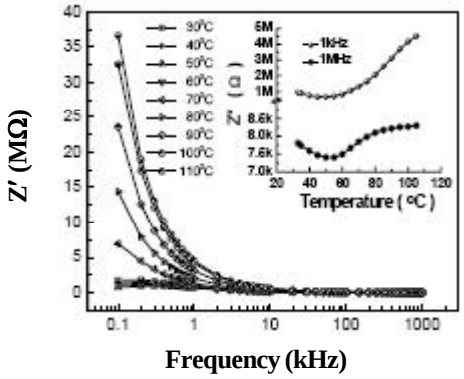

Figure 4: Frequency dependence of imaginary part of impedance of anthraquinone-0.6% alizarin at different temperatures. Inset: Temperature dependence of imaginary part of impedance at 1kHz and 1MHz

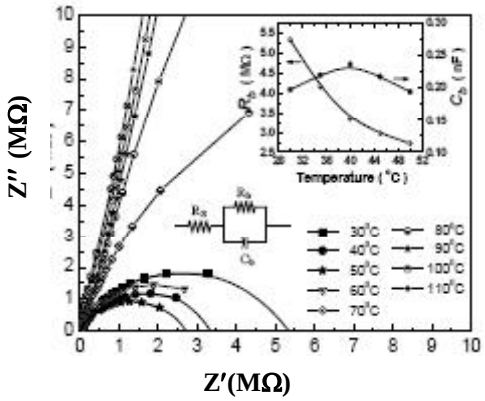

Figure 5: Complex impedance plots of anthraquinone-0.6% alizarin at different temperatures. Inset 1: Variation of R_b and C_b with temperature. Inset 2: Appropriate equivalent electrical circuit

variation of the real (Z′) and imaginary (Z″) part of impedance with frequency at different temperature. It is observed that the magnitude of Z′ decreases on increasing frequency. Inset of figures 3 and 4 respectively, display that the value of Z′ decreases with temperature up to 50^0C and afterwards it increases. This indicates a transition form the semiconducting state to the conducting state. This result is in consistent with the dielectric studies. The value of Z′ decreases with rise in temperature show negative temperature coefficient of resistance (NTCR) type behavior of AQAL. In other words, curves display an increase in ac conductivity with the increase in temperature (up to 50^0C) and frequency. This result may be related to the release of space charge as a result of reduction in the barrier properties of material with the rise in temperature and may be a responsible factor for the enhancement of ac conductivity of material with temperature at higher frequencies. The loss spectrum (Figure 4) is characterized by some important features in the pattern, such as (i) a decrease in Z″ without any peak in the investigated frequency range at high temperatures ($\geq 60^0$C), (ii) appearance of small peak (Z''_{max}) in the loss spectrum (up to 60^0C), (iii) typical asymmetric peak broadening with the rise in temperature and (iv) the values of Z''_{max} decrease and shift to higher frequencies with the increasing temperature. The asymmetric broadening of peaks in frequency explicit plots of Z″ suggests that there is a spread of relaxation times i.e. the existence of a temperature dependent electrical relaxation phenomenon in the material[13]. The spreading is indicated by the width of the curves. The merger of Z′ (Figure 3) as well as Z″ (Figure 4) values in the high frequency region may possibly be an indication of the accumulation of space charge in the material.

Figure 5 shows the complex impedance spectrum of AQAL measured at different temperature. It is observed that the complex impedance data is represented by depressed semicircle (i.e. centers of semicircle lie below the abscissa axis) in semiconducting region (solid symbols). The Debye's expression is modified in such situation by introducing a factor n. This modification leads to the Cole-Cole empirical behaviour described by the following equation[14]:

$$Z^*(\omega) = Z' + iZ'' = R/[1 + (i\omega/\omega_o)^{1-n}] \quad (1)$$

Full Paper

where n represents the magnitude of the departure of the electrical response from an ideal condition and can be determined from the location of the center of the Cole-Cole circles. This equation shows that the center of the semicircle obtained by data plotting in the complex plane is located below the real axis indicates the polydispersive non-Debye type dielectric relaxation. When n goes to zero {i.e. (1-n)→1}, Eqn.(1) reduces to the classical Debye's formalism where center of the semicircle should lie on the real Z′- axis. Least squares fitting to the complex impedance data give the value of n>0 at all the temperatures, suggesting the dielectric relaxation to be of non-Debye type. This may happens due to the presence of distributed elements in the material-electrode system[11] that results in the deviation from the pure semicircle in complex impedance plots. This indicates that Ag |AQAL| Ag structure behaves as non-ideal at these temperatures. Further, from 60^0C onwards, the slope of the curves increases and bend towards Z″-axis indicating decrease in conductivity with the rise in temperature. The resistance of bulk (R_b) can directly be obtained from the intercept on the Z′- axis. The bulk capacitances (C_b) can be calculated using the relation:

$$\omega \tau_b = \omega R_b C_b = 1 \quad (2)$$

where ω is the angular frequency at the maxima of the semicircle and τ_b is the bulk relaxation time. It is seen from inset 1 of figure 5 that the value of R_b decreases increase in temperature indicating NTCR character of AQAL while C_b riches a maxima. The impedance data at low temperature are represented by a semicircle which do not starts with origin (~1kΩ).

The circuit equivalent to this can be approximated by a parallel arrangement of R_b and C_b with a series resistance (inset 2 figure 5). Also, it is observed that the value of ω_m increases while τ_b decreases with the rise in temperature (inset Figure 6). The bulk dc conductivity was calculated using the relation:

$$\sigma_{dc} = l / S R_b \quad (3)$$

where l is the thickness and S is the surface area of the specimen. The activation energy is estimated from the variation of σ_{dc} as a function of 10^3/T (Figure 6). The conductivity of an organic semiconductor is expressed as[21]:

$$\sigma_{dc} = \sigma_o \exp(-E_g/2k_BT) \quad (4)$$

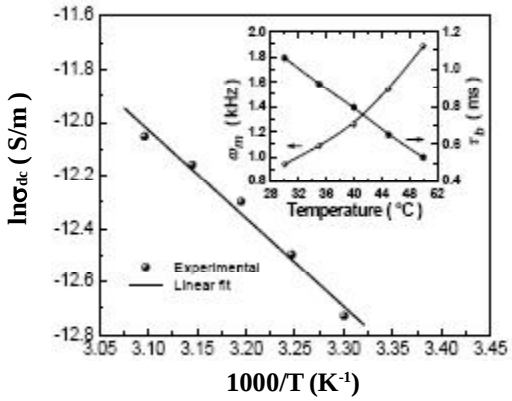

Figure 6: Temperature dependence of bulk dc conductivity of anthraquinone-0.6% alizarin. Inset: Variation of ω_m and τ_b with temperature Inset: Variation of ε with temperature at 1kHz and 1MHz

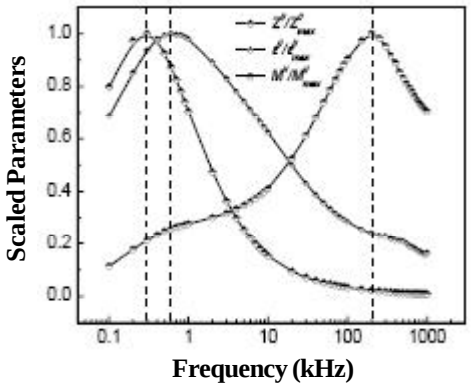

Figure 7: Normalized Z″, ε″ and M″ with frequency for anthraquinone-0.6% alizarin at 50ºC

where σ_o is a constant, E_g is the difference in energy between the highest point in the valance band and the lowest point of conduction band, k_B is the Boltzmann constant and T is the absolute temperature. A leaner least squares fitting of the experimental data to Eq.(4) given the value of E_g = 0.57 eV.

Figure 7 shows the variation of scaled parameters (Z''/ Z''_{max}, $\varepsilon''/\varepsilon''_{max}$ and M''/M''_{max}) with frequency at 50ºC, where ε″ is the imaginary part of dielectric constant. It can be seen that the peaks are not occurring at the same frequency ($f_{Z'} < f_{\tau'} < f_{M'}$). The magnitude of mismatch between the peaks of these parameters represents a change in the apparent polarization. The overlapping of peaks is an evidence of long-range conductivity whereas the difference is an indicative of short-range conductivity (via hopping type of mechanism)[22]. The value of FWHM (full width at half maximum) is found to be > 1.14 decades. These observations indicate that the distribution function for relaxation times is nearly temperature independent with non-exponential

conductivity relaxation. This phenomenon is well defined by a non-Debye type relaxation governed by the relation:

$$\phi(t) = \exp[-(t/\tau_m)^{\beta}] \; ; (0 < \beta < 1) \quad (5)$$

where ψ (t) stands for time evaluation of electric field within sample, $_m$ the conductivity relaxation time, β is the Kohlrausch exponent. The smaller the value of β larger the deviation of relaxation with respect to Debye type relaxation ($\beta = 1$).

A non-exponential type conductivity relaxation governed by the Eq.(5) suggests the possibility of ion migration that takes place via hopping accompanied by a consequential time-dependent mobility of other charge carriers of the same type in the vicinity occurs.

The ac electrical conductivity was obtained in accordance with the following relation:

$$\sigma_{ac} = (l/S).G(\omega) \quad (6)$$

where $G(\omega)$ is the conductance. The log-log plot of electrical conductivity versus frequency at different temperature (Figure 8) shows strong dependence on frequency as well as temperature. Also, the plots show an onset in semiconducting state with two different positive slopes (region I and II) indicating that σ_{ac} increases with frequency. The total ac conductivity of the compound can therefore, be written as $\sigma_{ac} = \sigma_I(\omega) + \sigma_{II}(\omega)$.

These are due to two different conduction mechanisms, described by σ_I (prevailing in region I) and σ_{II} (prevailing in region II). Also, the onset shifts towards higher side with the rise in temperature. The frequency variation of σ_{ac} found to obey universal behaviour:

$$\sigma_{ac} = A\omega^{s} \quad (7)$$

With $0 \le s \le 1$ and ω is angular frequency of applied ac field, in the frequency sensitive region. We find the value of s to decrease with the increasing temperature in semiconducting state and then it increases (inset figure 8). The model based on classical hopping of electrons over barrier[23] predicts a decrease in the value of the index s with the increase in temperature and so found to be consistent with the experimental results. Thus, the classical hopping of electrons may be the dominating mechanism in the system. This indicates that the conduction process is a thermally activated process.

Figure 9 shows the temperature dependence of ac conductivity. The nature of variation is almost linear, in semiconducting region and the value of E_a = 0.42 eV at

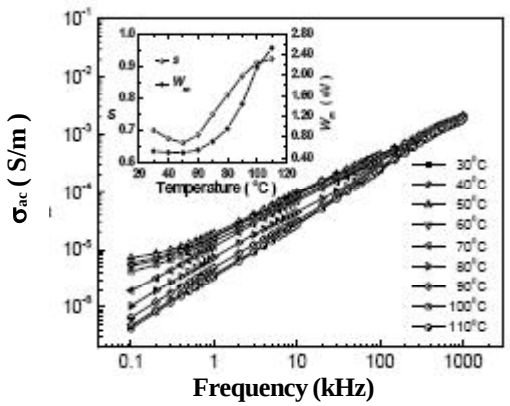

Figure 8: Variation of ac conductivity with frequency at different temperatures for anthraquinone-0.6% alizarin. Inset: Variation of index 's' and W_m with temperature

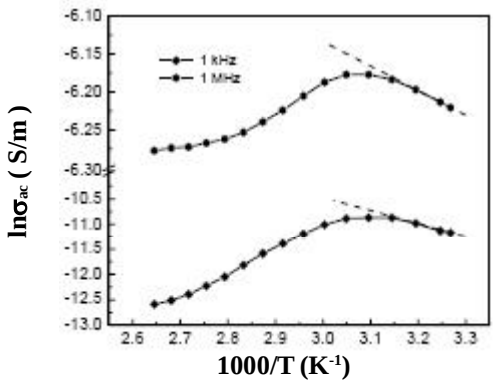

Figure 9: Temperature dependence of ac conductivity of anthraquinone-0.6% alizarin at 1kHz

1kHz obtained by least squares fitting of the data in semiconducting region using Eq.(4). Also, a decrease in the value of E_a (= 0.052 eV at 1MHz) has been observed. The low value of activation energy may be due to the carrier transport through hopping between localized states in disordered manner. These localized states may be the clusters of impurity ions and/or structural defects.

Using correlated barrier hopping (CBH) model[24], the binding energy has been calculated according to the following equation:

$$s = 1 - \beta \quad (8)$$

where

$$\beta = 6k_B T / W_m \quad (9)$$

where W_m is the binding energy, which is defined as the energy required to remove an electron completely from one site to the another site. The characteristic decrease in slope (inset figure 8) with the rise in temperature is due to the decrease in binding energy as illustrated in inset figure 8. From the values of the binding energy

minimum hopping distance R_{min} is calculated[25]:

$$R_{min} = 2e^2 / \pi \varepsilon_o \varepsilon Wm \quad (10)$$

where ε_o is the permittivity of free space and e is the electronic charge. Figure 10 illustrates that R_{min} increases with the increase in frequency at all the temperatures. Figure 11 shows the variation of R_{min} with temperature at various frequencies. It is observed that the values of R_{min} decreases up to transition temperature and then it starts increasing and at higher temperatures R_{min} again decreases.

In the hopping models ac conductivity behaviour in the higher frequency region where the conductivity increases the charge transport is dominated by contribution from hopping in finite clusters.

The ac conductivity data have been used to evaluate the density of states at Fermi level $N(E_f)$ using the relation[26]:

$$\sigma_{ac}(\omega) = (\pi/3)e^2\omega k_B T\{N(E_f)\}^2\alpha^{-5}\{\ln(f_o/\omega)\}^4 \quad (11)$$

where f_o the photon frequency and α is the localized wave function, assuming $f_o = 10^{13}$ Hz, $\alpha = 10^{10}$ m^{-1} at various operating frequencies and temperatures. Figure 12 shows the Frequency dependence of $N(E_f)$ at different temperature. It can be seen that the value of $N(E_f)$ decreases with the increase in operating frequency in semiconducting region and afterwards plots show minima which ultimately vanishes at higher temperatures and starts increasing with the increase in frequency. Figure 13 illustrates the variation of $N(E_f)$ with temperature at different frequency. It is seen that the plots show

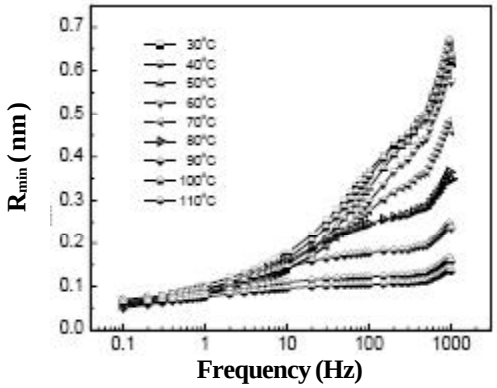

Figure 10: Frequency dependence of R_{min} of anthraquinone-0.6% alizarin at different temperatures

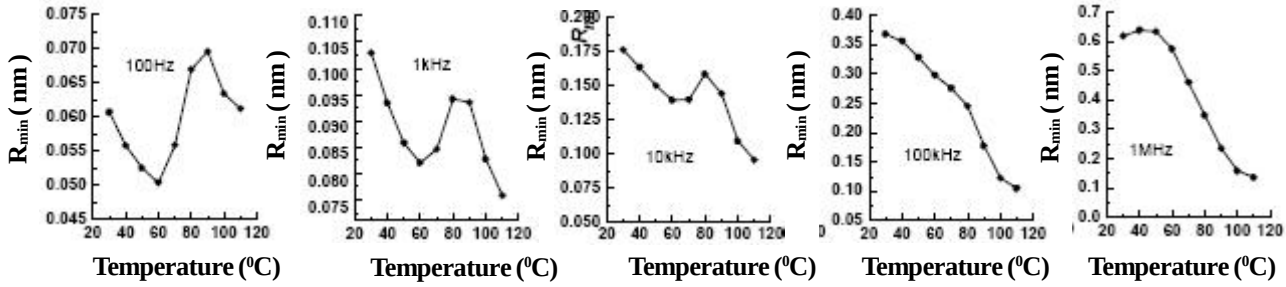

Figure 11: Temperature dependence of R_{min} of anthraquinone-0.6% alizarin at different frequencies

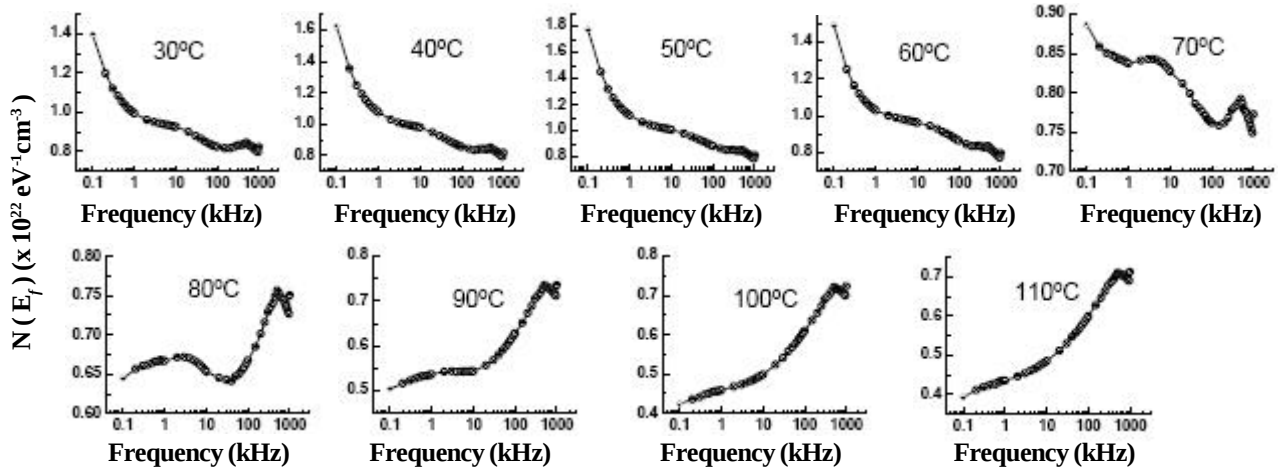

Figure 12: Variation of density of states at Fermi level with frequency at different temperatures for anthraquinone-0.6% alizarin

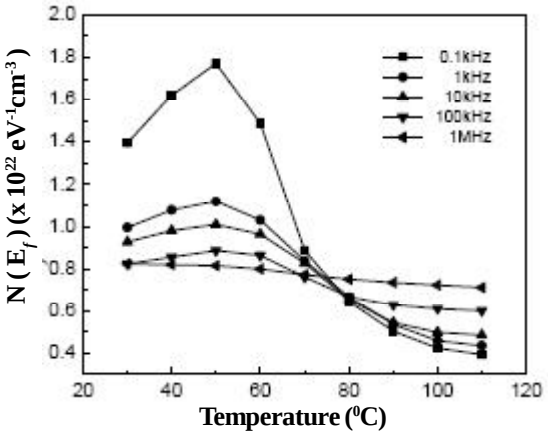

Figure 13: Temperature dependence of density of state at Fermi level of anthraquinone-0.6% alizarin at different temperatures

transition i.e. the value of $N(E_f)$ increases with the rise in temperature in semiconducting region and then it decreases. This result is in consistent with the dielectric and impedance studies.

CONCLUSIONS

This work reports the results of our investigation on the electrical properties of organic mixture anthraquinone-0.6% alizarin, a π-conjugated organic semiconductor, using complex impedance spectroscopy technique. The experimental results indicate that the compound exhibits (i) the NTCR character, (ii) a transition from semiconducting to conducting state, (iii) temperature-dependent relaxation phenomena, and (iv) non-Debye type dielectric relaxation. The ac conductivity obeys the power law and the dispersion in conductivity was observed in the lower frequency region. Also, the frequency dependent ac conductivity at different temperatures indicated that the conduction process is thermally activated process. The activation energy and density of states at Fermi level have been estimated from ac conductivity. Also, the system supports correlated barrier hopping model. Modulus analysis has indicated the possibility of hopping mechanism for electrical transport processes in the system with non-exponential-type conductivity relaxation.

REFERENCES

[1] D.Natali, M.Sampietro; Nuclear Instrum.Methods Phys.Res.A, **512**, 419 **(2003)**.
[2] F.Ebinawa, T.Kurokawa, S.Nara; J.Appl.Phys., **54**, 3255 **(1983)**.
[3] C.J.Drurg, C.M.J.Mustaers, C.M.Hart, M.Matters, D.M.Deleeuw; Appl.Phys.Lett., **73**, 108 **(1983)**.
[4] B.Crone, A.Dodabalapur, Y.Y.Lin., R.W.Filas, Z. Bao, A.Laduca, R.Sarpeshkar, H.E.Katz, W.Lin; Nature, **403**, 521 **(2000)**.
[5] S.H.Kim, S.C.Lim, J.H.Lee, T.Zyoung; Curr.Appl. Phys., **5**, 35 **(2005)**.
[6] C.W.Tang, S.A.Vanslyke; Appl.Phys.Lett., **51**, 913 **(1987)**.
[7] P.E.Burrows, S.R.Forrest, M.E.Thompson; Curr.Op.Solid State Mater.Sci., **2**, 236 **(1997)**.
[8] J.H.Schon, C.Kloc, A.Dodabalapur, B.Batlogg; Science, **289**, 599 **(2000)**.
[9] S.H.Kim, T.Zyoung, H.Y.Chu, L.M.Do, D.H. Hwang; Phys.Rev.B, **61**, 15854 **(2000)**.
[10] A.K.Jonscher; Dielectric Relaxation in Solids, Chelsea Dielectrics Press, London, **(1983)**.
[11] J.R.MacDonald; 'Impedance Spectroscopy: Emphasizing Solid Materials and Systems', John Wiley and Sons, NY, **(1987)**.
[12] C.K.Suman, K.Prasad, R.N.P.Choudhary; J.Mater. Sci., **41**, 369 **(2006)**.
[13] F.Yakuphanogulu, I.Erol; Physica B: Cond.Matter., **352**, 378 **(2004)**.
[14] J.C.Scott; J.Vac.Sci.Technol.A, **21**, 521 **(2003)**.
[15] G.Paasch; Synth.Met., **122**, 145 **(2001)**.
[16] M.A.Baldo, S.R.Forrest; Phys.Rev.B, **64**, 085201 **(2001)**.
[17] I.Thurzo, V.Nadazdy, M.Kumeda, T.Shimizu; J. Non-Cryst.Solids, **227**, 207 **(2000)**.
[18] H.Bässler; Phys.Stat.Sol.(b), **175**, 15 **(1993)**.
[19] K.P.Chandra, K.Prasad, R.N.Gupta; Physica B: Cond.Matter., **388**, 118 **(2007)**.
[20] C.M.Li, L.K.Pan, C.Q.Sun, J.Zhang, Dan Gamota; Proc.Contributed paper of NSTI Nanotechnology Conference and Trade Show, Anaheim, CA, USA, **3**, 165-168 **(2005)**.
[21] F.Gutman, L.E.Lyons; Organic Semoconductors, John Wiley and Sons, NY, **(1967)**.
[22] M.A.L.Nobre, S.Lanfredi; J.Phys.Chem.Solids, **64**, 2457 **(2003)**.
[23] S.R.Eilliot; Philos.Mag.B, **37**, 553 **(1978)**.
[24] S.Mollah, K.K.Som, K.Bose, B.K.Choudhri; J.Appl. Phys., **74**, 931 **(1993)**.
[25] R.Salam; Phys.Stat.Sol.(a), **117**, 535 **(1990)**.
[26] G.D.Sharma, Manmeeta Roy, M.S.Roy; Mater.Sci. Engg.B, **104**, 15 **(2003)**.